

MACHINE DEVELOPMENT STUDIES FOR PSB EXTRACTION AT 160 MEV AND PSB TO PS BEAM TRANSFER

V. Forte*, M.A. Fraser, S. Albright, W. Bartmann, J. Borburgh, L.M. Coralejo Feliciano, H. Damerau, A. Ferrero Colomo, D. Gamba, G. P. Di Giovanni, B. Mikulec, A. Guerrero Ollacarizqueta, M. Serluca, L. Sermeus, G. Sterbini, CERN, Geneva, Switzerland

Abstract

This paper collects the machine development (MD) activities for the beam transfer studies in 2016 concerning the PSB extraction and the PSB-to-PS transfer. Many topics are covered: from the 160 MeV extraction from the PSB, useful for the future commissioning activities after the connection with Linac4, to new methodologies for measuring the magnetic waveforms of kickers and dispersion reduction schemes at PS injection, which are of great interest for the LHC Injectors Upgrade (LIU) [1] project.

INTRODUCTION

Several MDs have been performed for the PSB-to-PS transfer and PSB extraction in 2016. The outcome of the studies has provided useful input for the hardware and beam study activities related to the LIU project. An exhaustive list is reported in Tab. 1:

Table 1: List of 2016 MDs

MD number	Description	Duration
88	PSB extraction at 160 MeV	2 days
1366	Recombination kickers waveforms measurements	>70 hours
1939	PS injection kicker (KFA45) waveform measurements	1 week
1904	PSB-BTi-BT-BTP-PS dispersion measurements	few slots
1829, 1893	LHC "long bunches" transfer and emittance evaluation	3 days
1928	Sanity tests of sem-grids after PS injection	5 hours
1769	Automatic alignment in the BTi-BT-BTP at PS injection	2 days
1740	Septum SMH42 new position and angle	0.5 days

MD88: PSB EXTRACTION AT 160 MEV

The extraction of the beam at 160 MeV is foreseen during the commissioning activities after the connection with Linac4. The intent is to inject and extract the beam to the dump in the beam transfer measurement (BTM) line and to avoid losing it all in the PSB during the commissioning phases. This possibility will facilitate initial injection checks and procedures at low energy, before the energy ramping phase [2]. For this reason it was important to prove the feasibility of such an extraction.

The MD was executed in 2 non-consecutive days in dedicated mode, as the power supplies of extraction septum and quadrupoles in the transfer lines cannot switch between 160 MeV and 1.4 GeV operations. The MD required coordination of experts between different groups, in order to relax the hardware and software interlock settings to operate the extraction at 160 MeV.

Initial setup and beam preparation

Initial optics simulations have been performed by W. Bartmann [3]. The cycle at 160 MeV up to extraction was prepared in advance and is shown in Fig. 1. The radio-frequency (RF) settings from LHC25 on PSB Ring 3 were used.

* vincenzo.forte@cern.ch

Many experts were involved and coordinated to perform modifications in the transfer line for the 160 MeV extraction (~ 27 % of the nominal magnetic beam rigidity at 1.4 GeV). In particular, they had to: modify the tolerances in the power supply, modify tolerances on the controls side and reduce limits for the extraction kicker (to 7 kV) and of the extraction bumpers (to +100 A), go locally to modify the limit for the extraction bumpers and change the interlock level for the extraction kicker (7 kV). The beam position monitors

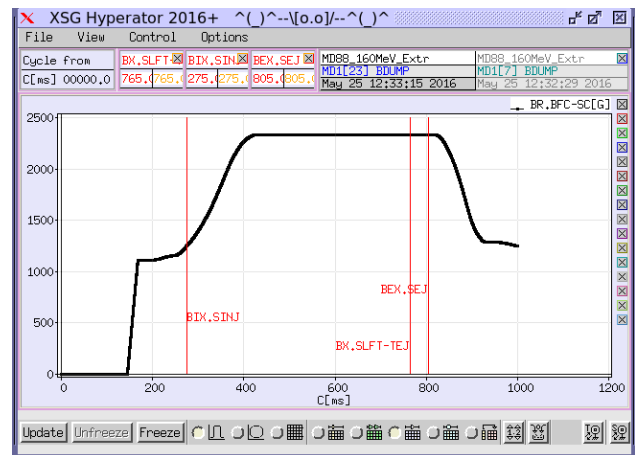


Figure 1: The PSB magnetic cycle at 160 MeV up to extraction (time marker “BEX.SEJ”, at ~ 805 ms).

sum signals along the beam transfer (BT-BTM) line to the dump (sketched in Fig. 2) were used to monitor step-by-step the beam threading in the line, while the evaluation of the transmission efficiency was performed through beam current transformers (BCTs) in the PSB ring (just before extraction) and at the end of the line (BTM.BCT10).

Conclusions of the MD

The final configuration was obtained by extending orbit correction functions to extraction, rescaling angle/position correctors, extraction bumpers (to 140 A, only in local mode), kicker (12 kV) and septum (1862 A), and by re-steering the line through the trajectory corrections. A transmission efficiency of ~ 80% to the dump was finally reached with a bunch of 60×10^{10} p, $(\delta p/p)_{rms} = 1.6 \times 10^{-3}$ and 474 ns total bunch length, as shown in Fig. 3.

The longitudinal beam profiles, trajectories and losses through beam loss monitors (BLMs) along the extraction line are shown in Fig. 4. Some issues remain to be investigated, like observed jitter on the synchronisation between the extraction kicker and beam, leading occasionally the beam to be extracted in two turns, and the losses in transfer line, probably related to limited acceptance and non-optimal trajectories (especially at higher intensities). These issues

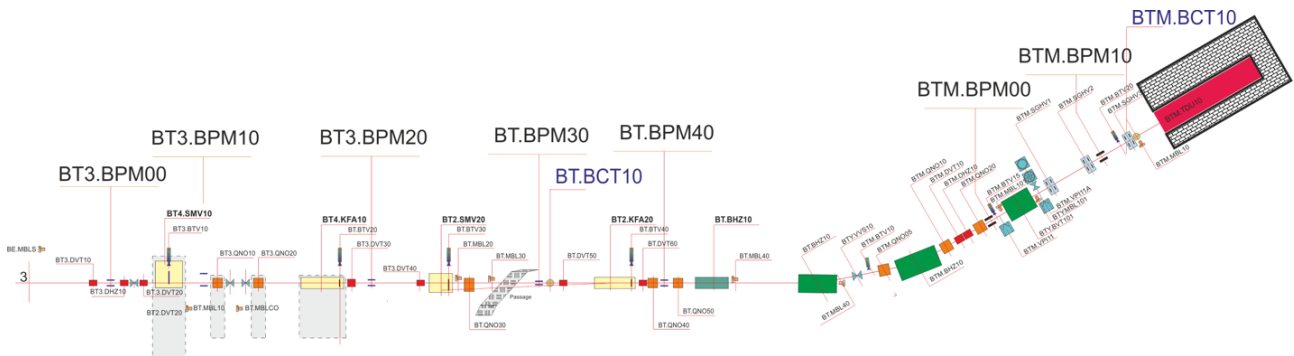


Figure 2: The transfer line (BT-BTM) from the PSB Ring 3 to the beam dump. The BPMs and BCTs are labelled with larger fonts (edited from [4]).

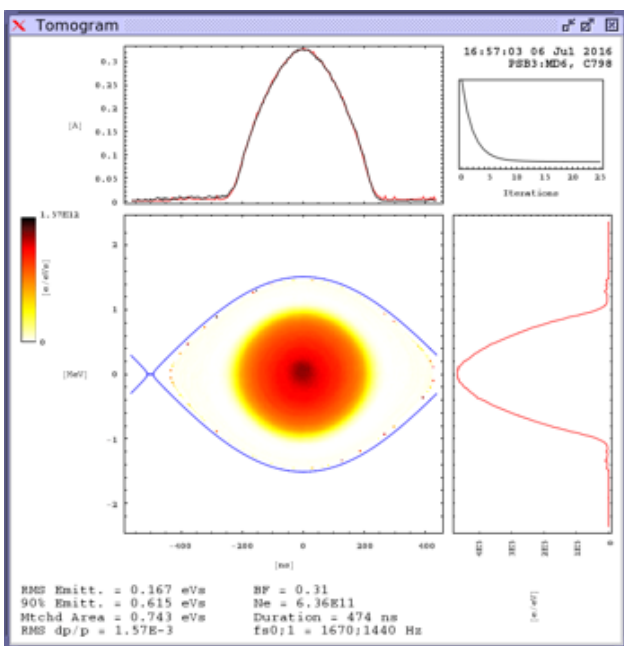


Figure 3: The tomographic reconstruction of the longitudinal phase space for the extracted bunch at 160 MeV.

should deserve more attention in order to try and achieve more than 80% transmission efficiency. However, the limited commissioning phase of extraction at 160 MeV foreseen during the PSB-Linac4 connection has steered the repetition of this dedicated MD in 2017 toward a lower priority.

MD1366: NEW BEAM-BASED MEASUREMENTS OF PSB-TO-PS VERTICAL RECOMBINATION KICKERS [5]

The increased bunch length demanded by the LIU project to mitigate emittance growth from space-charge on the PS injection plateau puts strong constraints on the rise-times of the recombination kickers in the transfer lines between the CERN Proton Synchrotron Booster (PSB) and the Proton Synchrotron (PS). A beam-based technique has been developed to validate the waveforms of the recombination kickers. High-resolution measurements are presented by extracting the intra-bunch deflection along bunches with lengths comparable to or longer than the rise-time of the kicker being

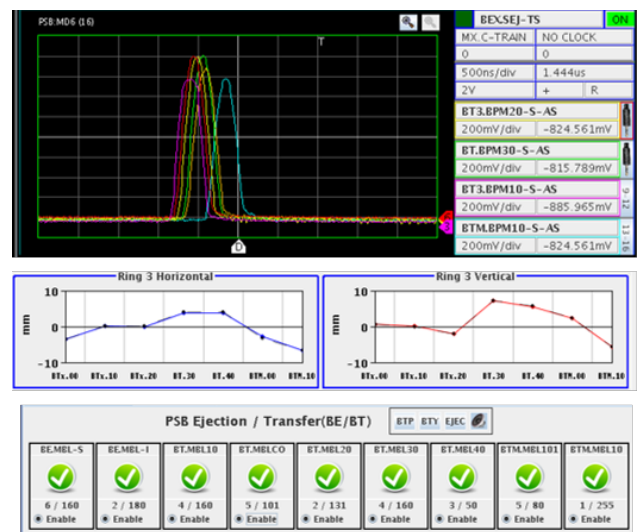


Figure 4: Longitudinal beam profiles (top), ejection trajectories (centre) and BLM levels (bottom).

probed. The methodology has been successfully applied to the three vertical recombination kickers named BT1.KFA10, BT4.KFA10 and BT2.KFA20, and benchmarked with direct measurements of the kicker field made using a magnetic field probe. This paper describes the beam-based technique, summarises the main characteristics of the measured waveforms, such as rise-time and flat-top ripple, and estimates their impact on beam brightness.

The BT1.KFA10, BT4.KFA10 and BT2.KFA20 kicker magnets are used to recombine the bunches coming from the four vertically-stacked rings of the PSB. The batch, constituted by several bunches, can then be directed to the dump at the end of the beam transfer measurement (BTM) line, or to the ISOLDE experiment, or to the PS through the BTP line. The single bunches going to the PS for the LHC (Standard production) are of interest for this paper. To preserve the brightness of the LHC bunches it is very important that the recombination does not disturb the vertical distribution of particles of the bunches.

The present LHC baseline (standard production) is constituted by 180 ns long bunches, spaced by 327 ns, at 1.4 GeV. The bunches, coming from different PSB rings, are labeled as "Rx", where x is the PSB ring number from which they are ejected. The LHC injections into the PS are performed with two batches separated by 1.2 s. i.e. the PSB basic period. In

the first PS injection four bunches are extracted from each ring in the following sequence: R3 → R4 → R2 → R1. The second injection is composed of two bunches: R3 → R4.

BT4.KFA10 recombines R3 (un-kicked) and R4 (kicked), BT1.KFA10 recombines R2 (un-kicked) and R1 (kicked), and finally, BT2.KFA20 recombines R3-R4 (un-kicked) and R2-R1 (kicked), as shown in Fig. 5.

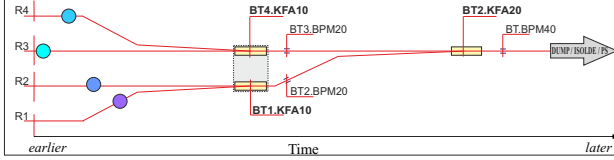


Figure 5: A simplified sketch (edited from [4]) of the recombination kickers in the BT-BTP line (lateral view) and the sequence of PSB bunches before being recombined.

The recombination kickers are triggered in the time between two adjacent bunches. A relatively short rise-time is important to avoid that the transient of the magnetic field perturbs the tail of the first bunch and/or the head of the second one. In order to obtain a clean transfer for the longer 220 ns LIU bunches, the specification [6] requires the 2-98% rise-time ≤ 105 ns.

The flat-top ripple of the kicker waveforms must be controlled to avoid the detrimental effects of vertical intra-bunch motion that will result in vertical emittance growth and filamentation in the PS. The specification requires ≤ 2% flat-top ripple for each recombination kicker.

These limits have to be considered without any further margin and are directly related to the emittance blow-up, which is expected from simulations [7] to be in the order of 2%.

Measurement set-up

The reconstruction of the kicker waveform was obtained from the measured displacement of the beam after it is kicked. In fact, the displacement δ at any beam position monitor (BPM) is directly proportional to the integrated magnetic field seen by the beam, such that the deflection angle θ at the kicker can be written as shown in Eq. 2:

$$\delta_{x,y} \propto \theta_{x,y} = \frac{e}{p} \int_0^L B_{y,x} dz \quad (1)$$

where p is the momentum, e is the electric charge, B is the magnetic field, L is the magnetic length and x , y , z are the horizontal, vertical and longitudinal coordinates respectively.

The first downstream BPM after each kicker was used to retrieve the beam displacement information in time, by taking the ratio between the vertical difference (Δ_y) and the sum (Σ) signals in a defined gating time window around the peak current location of the bunch. The BPM signals were monitored on an OASIS scope [8] in the control room and recorded as a function of the delay imposed on the kicker trigger.

Figure 6 shows an example of the sum and difference signals of BT.BPM40, which is the first downstream of BT2.KFA20. It is possible to distinguish different cases in the figure where (left) the first bunch (R4) is partially affected by the kick and R2 is fully kicked. the nominal case

(centre) where R4 is un-kicked and R2 is fully kicked and (right) the case where the second bunch (R2) is partially kicked and R4 stays un-kicked.

Figure 6 also shows the magnet input current signal of the BT2.KFA20 kicker on OASIS. It should be stressed that this last signal represents the input current for the magnet and is not representative of the magnetic waveform of the kicker. Moreover the current signal appears low-pass filtered due to the attenuation in its transmission to the OASIS scope and thus is only useful to determine and verify the delay applied to the trigger of the kicker.

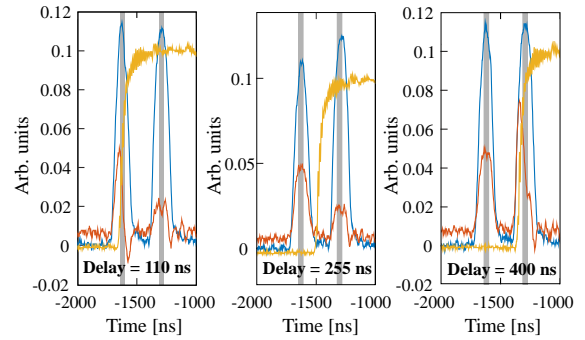


Figure 6: The BPM Δ_y (orange) and Σ (blue) signals, together with the current signal (yellow) for three different values of the BT2.KFA20 delay. The grey error-band is the chosen gating window around the peak current.

Measurement procedure

Calibration It is important to perform a beam-based calibration of the BPM with respect to the kicker voltage at the beginning of every measurement, as shown in Fig. 7. The calibration has to be performed in a nominal regime, i.e. with the first bunch completely un-kicked and the second one fully kicked, as in Fig. 6 (centre). Due to trajectory differences in the transfer line, the BPM signals of the two bunches have to be vertically shifted by an offset in order to be both aligned to the same reference. As shown in Fig. 6 (centre), the offset corresponds, for the fully kicked bunch, to the constant term of the linear regression of the measured deflection per kicker voltage, and, for the un-kicked bunch, to the average value.

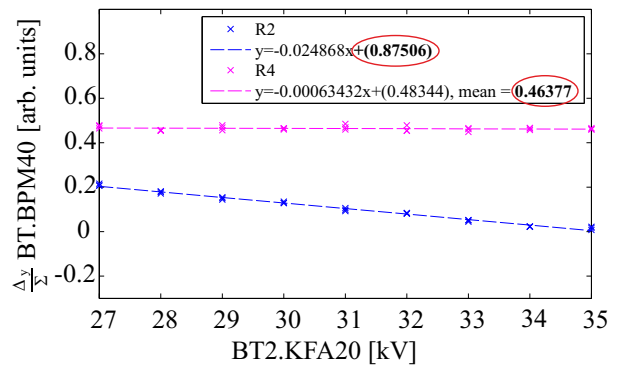


Figure 7: The calibration plot for the BT2.KFA20 kicker vs BT.BPM40 (the offsets are in the red ellipses).

Reconstruction The measurement was performed by scanning the fine delay of the recombination kicker and acquiring BPMs signals of the two consecutive bunches. The measured signal is shown in Fig. 8 (left). The reconstruction was then completed through the vertical shift of the two waveforms determined in the aforementioned calibration process. After further statistical processing the waveform is shown in Fig. 3 (right) plotted with 1 standard deviation (SD) significance bounds. As the BPM responses are more

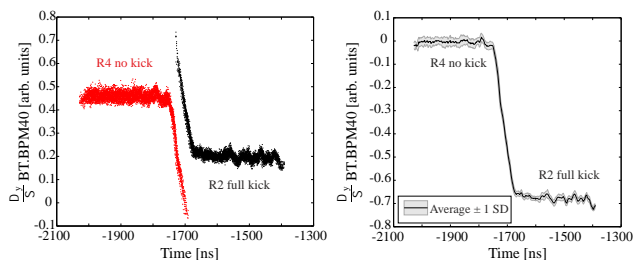


Figure 8: The magnetic waveform reconstruction process.

precise at high currents [7], the bunch population at the exit of the PSB was chosen at $\sim 200 \times 10^{10}$ protons and, owing to the length of the bunches (180 or 220 ns), multiple intra-bunch measurement samples could be taken within individual bunches. This allowed high granularity in the measurements.

The characteristics of the waveform were only measured at the relevant locations where the bunches sit, very close to, and either side of, the rising edge. For the BT1(4).KFA10 the flat-top ripple is relevant during only the first 220 ns before and after the rising edge as single bunches are recombined. For BT2.KFA20 up to ~ 550 ns (from one 220 ns bunch length plus 327 ns bunch spacing) is important, as it recombines doublets (R3-R4 and R2-R1).

The beam-based reconstructions were performed at the present operational voltages for an extraction energy of 1.4 GeV from the PSB, corresponding to: 43 kV for BT1(4).KFA10 and 27 kV for BT2.KFA20. At the future 2 GeV extraction energy (+30% magnetic rigidity) the kickers will require 56 kV for BT1(4).KFA10 and 35 kV for BT2.KFA20.

The magnetic field measurements using a magnetic measurement coil for the KFA20 kickers were performed at 27 kV on the magnets installed in the machine during a technical stop, while the others were done at 50 kV for BT1.KFA10 (in the machine) and 56 kV for BT4.KFA10 (in the lab). These measurements were then scaled-up to be compared with the beam-based measurements. This comparison is valid in the assumption of an ideal "linear" response of the kicker system, which was demonstrated in dedicated beam-based measurements [7].

Measurement results

The raw measurement data was filtered using a (low-pass) median filter with a time window of 10 ns. This choice was made to smooth the signal whilst at the same time keeping a large enough bandwidth to observe any significant frequency components. The beam-based measurements could be compared with the magnetic measurements from fast magnetic measurement coils, in the machine and/or in the lab.

BT1.KFA10 The beam based measurements, shown in Fig. 9, indicate the presence of ripple and an initial overshoot that is filtered by the field measurement probe whose characteristics are unknown. The measurement results from the probe appear low-pass filtered and do not present the initial overshoot.

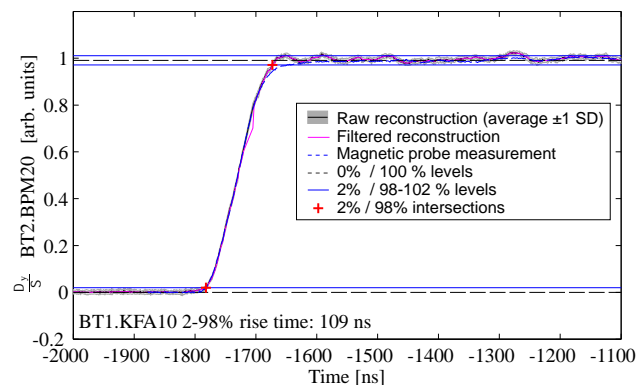


Figure 9: BT1.KFA10 waveform vs. probe in the machine.

BT4.KFA10 The comparison between the beam-based and lab-based measurements are shown in Fig. 10. A slight disagreement is visible in the amplitude of the flat-top ripple and might be induced by the fact that only one of the two modules of the kicker was probed and the system was not exactly equal to the one installed in the machine.

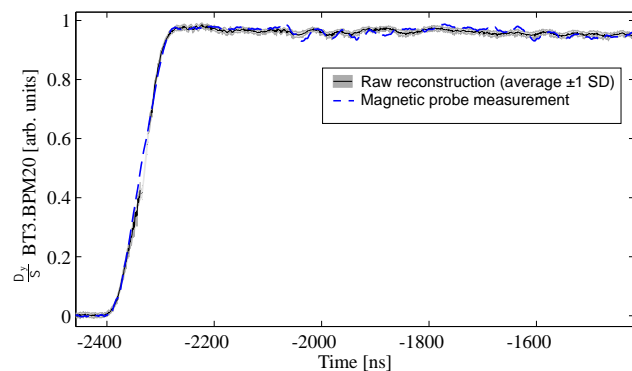


Figure 10: BT4.KFA10 waveform vs. probe in lab.

BT2.KFA20 The beam-based measurements were compared with the measurements from a fast and more reliable magnetic field probe, which was inserted directly inside the magnet in the machine. The results, in Fig. 11, show an excellent agreement. The flat-top peak ripple is confined inside $\pm 2\%$, except for a reflection inside the black dashed ellipse. The ripple induced from this reflection creates some undesired vertical emittance blow-up, and the KFA20 system will be recabled into the same configuration as KFA10 as part of the LIU project to remove this reflection.

Rise-times, flat-top ripples, frequency responses The rise-time and flat-top ripples estimated from the beam-based measurements, which are summarised in Tab. 3, are just in specification.

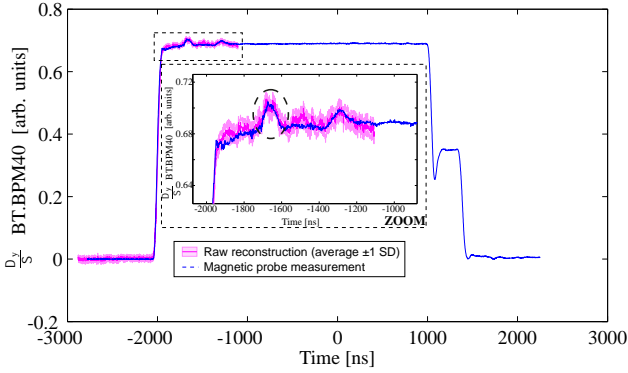


Figure 11: The BT2.KFA20 beam-based magnetic waveform.

After considering all the error sources such as the BPM sensitivity to current, the calibration technique, the beam reproducibility, the jitter of the firing trigger of the kicker, etc., the tolerance on the final rise-time measurements was conservatively set to ± 10 ns and the lab-based field measurements validated.

Table 2: The rise-times and flat-top ripples

	2-98% rise-time [± 10 ns]	Flat-top ripple \hat{B}/\bar{B} [%]
BT1.KFA10	109	2
BT4.KFA10	104	2
BT2.KFA20	105	2

In order to have high resolution needed for a fast Fourier transform (FFT), a detailed flat-top measurement was necessary. From the measurements in Fig. 12 the frequency components that need correction by the PS transverse feedback could be assessed: there is no significant component measured over 20 MHz (-3 dB bandwidth of the feedback). Moreover, the applied median filtering reproduced well the main frequency components of the raw signal.

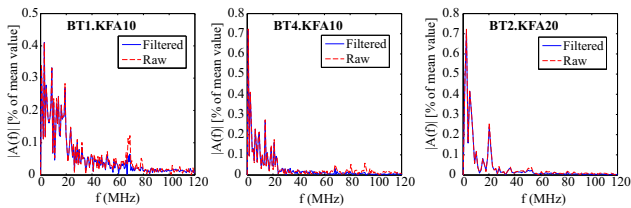


Figure 12: The measured frequency spectra of the flat-top ripple for BT1.KFA10 (left), BT4.KFA10 (centre) and BT2.KFA20 (right).

Conclusions of the MD

A new method to measure the magnetic waveform of the recombination kickers BT1(4).KFA10 and BT2.KFA20 was introduced. This method is valid for measurements in transfer lines where the waveform transients are comparable to the bunch length of the beam being used as a probe. The waveforms have been benchmarked with direct magnetic probe measurements, showing excellent agreement for all the kickers measured. The measured rise-times and flat-top ripples appear just within specification. The frequency components of the kickers are within the PS transverse feedback -3 dB bandwidth specification. Simulations of the incurred

emittance growth using the measured waveforms show a blow-up per ring up to 2.3% (summing in quadrature the contribution of each kicker) for 220 ns bunch lengths and 327 ns bunch spacing at 1.4 GeV [7]. Hardware modifications are on-going inside the framework of the LIU project to reduce the BT2.KFA20 ripple and increase the operational voltage margin at 2 GeV by recabling it as the KFA10.

MD1939: BEAM-BASED WAVEFORM MEASUREMENTS OF THE CERN PS INJECTION KICKER [9]

The KFA45 is the horizontal PS injection kicker used to transfer bunches from the BTP transfer line into the PS ring. During a PS cycle for the LHC, the kicker is fired at two instances in time spaced by 1.2 s, in order to fill the machine with a double-batch injection at 1.4 GeV from the PSB.

The four kicker modules have two modes of operation, linked with the termination impedance: terminated mode (TM), i.e. with a matched non-zero load impedance, and short-circuit mode (SC). Before 2017, the kicker was usually operated in TM and the SC mode was used only to compensate the missing current in case of module failures. The SC allows the doubling of the current going through the magnet and thus providing twice the kick. Since 2017 the KFA45 has been permanently configured in SC. In order to guarantee a clean transfer to the PS, the 2-98% rise and fall times and the 2% flat-top ripple of the KFA45 waveform must respect the specification [6], i.e. ≤ 105 ns and $\leq 2\%$ respectively.

Beam-based measurements of the KFA45 waveform are necessary because they represent the only way to retrieve the magnetic waveform of the installed system, required to confirm the kicker performance for LIU. A direct measurement with a field probe is very complicated to perform as it would require the movement of two main bending units in the PS.

Experimental method

The reconstruction of the kicker waveform is obtained from the displacement δ of the beam once it is kicked. In fact, δ at any subsequent beam position monitor (BPM) is directly proportional to the integrated magnetic field seen by the beam and to the deflection angle θ imposed by the kicker, as shown in Eq. 2:

$$\delta_{x,y} \propto \theta_{x,y} = \frac{e}{p} \int_0^L B_{y,x} dz \quad (2)$$

where p is the momentum, e is the electric charge, B is the magnetic field, L is the magnetic length and x , y , z are the horizontal, vertical and longitudinal coordinates respectively. A fast BPM, in section 02 (BPM02) [10], was used to retrieve the beam displacement information, by taking the ratio between the difference and the sum signal at the peak current location of the bunch. The kicker and the BPM signals were monitored and recorded from an OASIS scope [8].

The waveform measurements were made using the second instance of the kicker (~ 1 μ s pulse length), which was delayed from the injection plateau to the extraction flat-top at 26 GeV. The increased rigidity of the circulating beam permitted measurements to be made and the beam extracted to an external dump without significant beam losses.

The measurement method is based on the observation of the beam's displacement at a given time after it fires. A large number of cycles (occurrences) containing a single bunch were analysed to probe the entire waveform by shifting the delay between the circulating beam and kicker trigger, covering the whole revolution period in the PS.

A challenging issue was the asynchronous triggering of the kicker with respect to the circulating beam at flat-top energy; the injection kicker timing is only designed to be synchronous with the beam at injection energy. The asynchronous triggering induced a pseudo-randomisation of the shift in time of the beam with respect to the kicker delay. Figure 13 (left) shows the large amount of cycle occurrences that were required in order to cover uniformly the $2.1 \mu\text{s}$ revolution period in the PS. By imposing an initial shift on the KFA45 trigger of 5 ns/occurrence, and repeated at finer steps of 2 ns/occurrence, inside a span of 340 ns, the beam jittered with respect to the KFA45 trigger, which led to an uncontrollable granularity of the occurrences for a defined sampling time. The kicker trigger reference was also oscillating in the absolute reference of the OASIS scope: the jittering of the magnet input current signals with a defined signal threshold for every occurrence is shown in Fig. 13 (right).

The synchronisation issue is being solved for future measurements by adding another timing from which the injection kicker can be triggered synchronously with the beam at all energies.

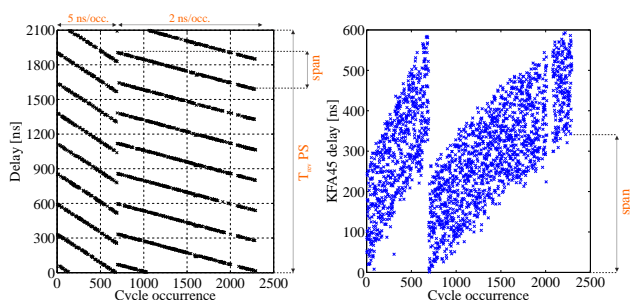


Figure 13: Beam (left) and KFA45 (right) delays.

Experimental results

A nominal single LHC bunch ($\sim 10 \times 10^{10}$ p) was used as a probe for the measurement, because it represented a good compromise between signal readability (for the BPM) and reduced losses at extraction.

Measurements were performed for TM and SC modes. The kicker total voltage was set equivalent to 270 kV. In TM all the four modules of the kicker were on, sharing the voltage, while in SC modules 1 and 2 were switched off, leaving modules 3 and 4 to work in short-circuit in order to compensate the missing current.

For every cycle, the closed orbit (CO) was approximated through a sinusoidal fit of the turn-by-turn position before the kick (through Eq. 3) and used to correct the baseline from the raw signal, as shown in Fig. 14. The residual signal from this difference was then considered for the reconstruction.

$$CO_{fit}(t) = A_0 + |A_1| \sin(2\pi f t + \phi_0) \quad (3)$$

The following parameters, shown in red in Eq. 3, are the free ones of the fit: A_0 is the measurement offset. A_1 is the

closed orbit amplitude, f is the horizontal frequency of the beam correlated to the horizontal betatron tune and ϕ_0 is the initial phase in the constant gating window around the kicker trigger. Systematic changes are observed in Fig. 15 where changes to the cycling of the machine during the long measurement campaign of many hours are evident and cannot be attributed to random errors. The signal recon-

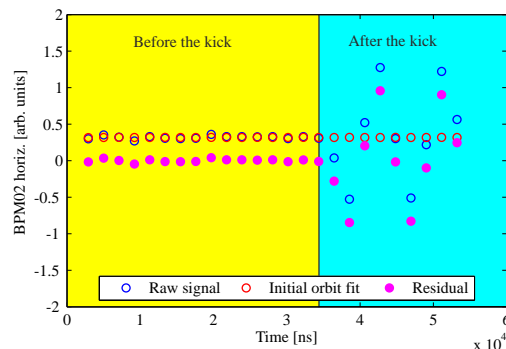


Figure 14: The BPM reading in time before and after the kick.

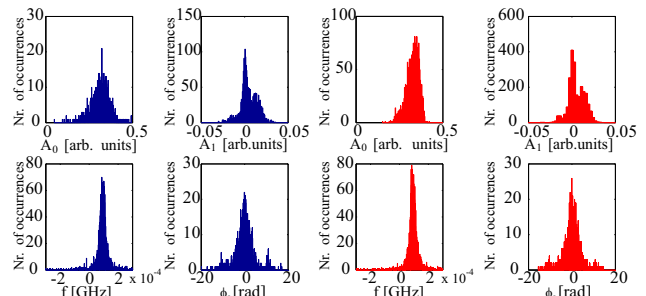


Figure 15: The distribution of the free fitting parameters for the measured occurrences in SC (blue) and TM (red).

struction, obtained by combining the occurrences, produces a waveform whose amplitude oscillates for nine times in the observation window at the horizontal betatron frequency of the machine, as shown in Fig. 16. The following analysis is

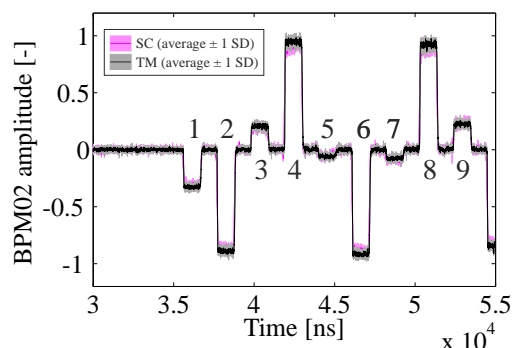


Figure 16: The numbered oscillations of the kicker waveform.

performed on the oscillation No. 2, as it presents the highest signal-to-noise ratio. The non-linearity of the BPM is being investigated, and the initial offset in the BPM before the kick appears to make oscillation No. 4 quite noisy.

Low-pass filtering and comparison with current measurements One can distinguish the measurements performed in TM and SC modes, as shown in Fig. 17. The signal has been low-pass filtered to smooth the measurement noise. Filtering was needed due to the poor granularity of the measurements. A moving average filter was applied with window sizes of 10 ns and 25 ns.

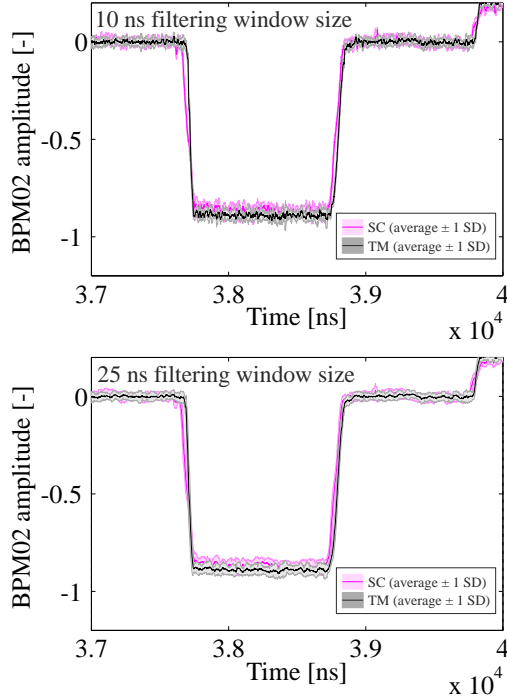


Figure 17: The (low-pass filtered) reconstructed waveforms.

Figure 18 shows the sum of the currents of modules 3 and 4, compared with the measured magnetic field waveforms.

The integrated magnetic field has a low-pass behaviour (both in SC and TM modes), not showing the ~ 20 MHz damped ripples shown in the current, related to the overshoot at the end of the rise time and to the reflection after ~ 600 ns of flat-top.

In SC mode the current rise and fall times are sharper than the measured magnetic field because of the the location of the current measurement point at the short circuit node downstream the magnet [11]. The rising and falling edges of the measured magnetic waveforms show an inflection: faster at the beginning of the rise and slower at the end. This phenomenon is related to the filling time of the magnet, which, in SC mode, is typically almost doubled due to the reflection of the current [11].

In TM mode, the excellent agreement between the current and beam-based magnetic measurements for both time constants confirms a good choice of the filtering.

Rise and fall times, flat-top ripple The evaluations of rise and falling times and flat-top ripple are shown in Fig. 19. 2-98% levels were computed with 25 ns time window filtering for TM, while, due to the more noisy data, a smaller interval, precisely 2.7-97.3%, has been considered for the SC. The values of rise and falling times correspond to the distances between two consecutive intersections at the bottom (top) and the top (bottom) edges of the waveform. The

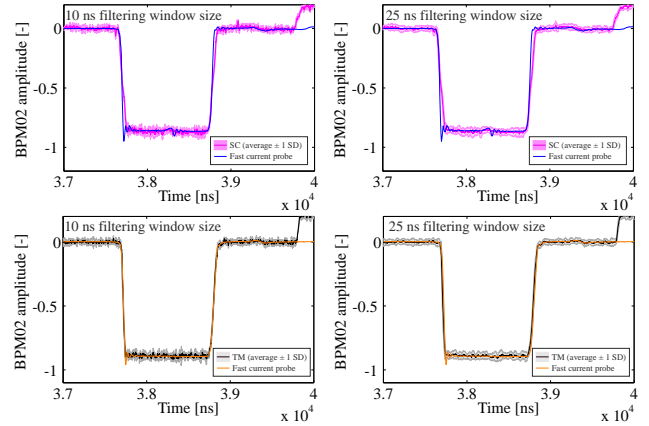


Figure 18: Reconstructed waveforms vs. currents.

values of flat-top ripple correspond to the maximum deflection, all along the flat-top, with respect to the flat-top average amplitude. Due to the filtering process and to the precision

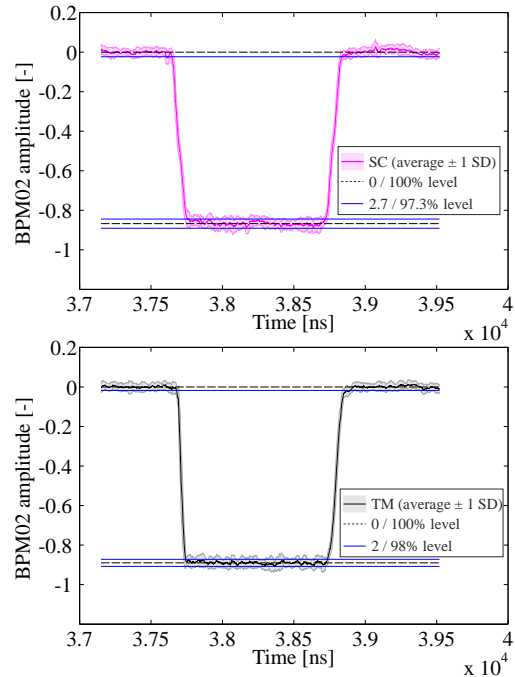


Figure 19: The rise and falling times evaluations.

level of the measurements, a ± 10 ns tolerance is considered on top of the reported values, as an educated guess. The results are summarised in Tab. 3.

Table 3: The rise and fall times and the flat-top ripple values for filter window sizes of 10 ns (and 25 ns in round brackets). Some values could not be determined (n.d.). *2.7-97.3% evaluation

KFA45 mode	Rise time [± 10 ns]		Fall time [± 10 ns]		Flat-top ripple (%)
	5-95%	2-98%	95-5%	98-2%	
SC	89 (92)	n.d. (104*)	93 (98)	n.d. (110*)	4.6 (2.7)
TM	46 (53)	n.d. (63)	96 (102)	n.d. (134)	3.3 (2.1)

Conclusions of the MD

An extensive MD campaign has been carried out to perform beam-based measurements of the magnetic waveform

of the PS injection kicker KFA45. These measurements were necessary to assess today's performance and that required by LIU in the future, and represent the only way to by LIU and present to date, the only way to probe the waveform of the magnet without moving other PS elements.

Measurements have been performed both in terminated (TM) and in short-circuit (SC) modes, which is the baseline configuration from 2017. The measurements in bunched mode showed rise times just consistent with specifications for SC mode. More measurements are, nevertheless, needed to investigate the flat-top ripple and improve precision. For this purpose, a new beam synchronous trigger will be used to improve the sampling. These new measurements will be performed in MD in 2017, profiting from the hardware improvements [12].

MD1904: PSB-BT-BTP-PS DISPERSION MEASUREMENTS AND RE-MATCHING

One of the main priorities of the transfer between PSB and PS for the LIU project is to have a matched optics in order to preserve the brightness between the PSB extraction and PS injection. In particular, the dispersion mismatch at PS injection is important. Analytical calculations [13] show that the dispersion mismatch can cause for standard (long) LHC bunches an horizontal emittance blow-up up to 10 (30)% for LHC25 and 20 (65)% for BCMS beams. The betatron mismatch is up to 5%.

A matched optics from the 4 PSB rings is foreseen after LS2 with the installation of a new quadrupole in the BTP line: this will allow to obtain a negligible horizontal blow-up due to dispersion mismatch, while the vertical blow-up will be up to 15% for long BCMS bunches. In the future the betatron mismatch is supposed to be negligible.

The dispersion was measured in the PSB ring, in the extraction line and in the PS ring (1st turn).

As an example of in the PSB Ring 3, a dispersion measurement is shown in Fig. 20 (other measurements in the PSB rings can be found in [14]). The dispersion at the PSB horizontal wirescanner measurements showed a value of -1.38 m, i.e. 5% less than the operational value of -1.46 m. This is an important indication for measurements on beams like BCMS, where the dispersive component on the emittance is particularly relevant.

The dispersion in the extraction lines showed an excellent agreement with the model [16] for the PSB outer rings (1 and 4), while for the inner ones (2 and 3) a difference up to 0.5 m was present, as shown in Fig. 21.

Present measurements of emittance growth at PS injection [15] show more than 20% emittance growth for BCMS beams. A new optics was calculated using MadX [17] in order to reduce the dispersive mismatch at PS injection and disentangle the contribution of the horizontal dispersion on the emittance growth at PS injection from other possible causes (e.g. space charge). The re-matching was performed by using the quadrupoles in the BT line, as they can be changed for every PSB user in parallel operation. The strengths for the present and re-matched optics are represented in Tab. 4. The new optics was tried in operation at the 1st turn in the PS ring.

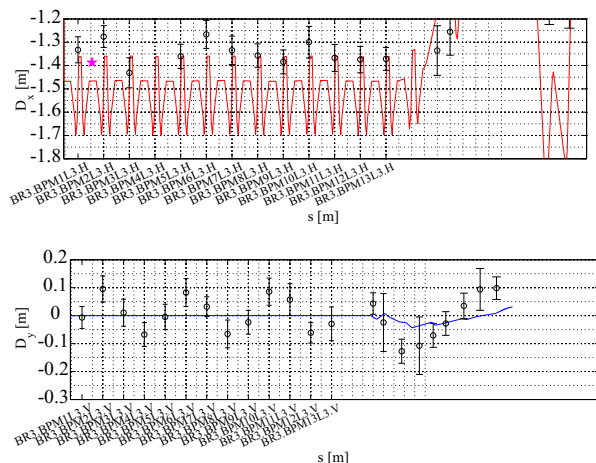


Figure 20: PSB Ring 3 dispersion in the horizontal (top) and vertical (bottom) planes (measurements - circle marker, model - solid lines). The measured horizontal wirescanner dispersion is represented by a magenta star on top.

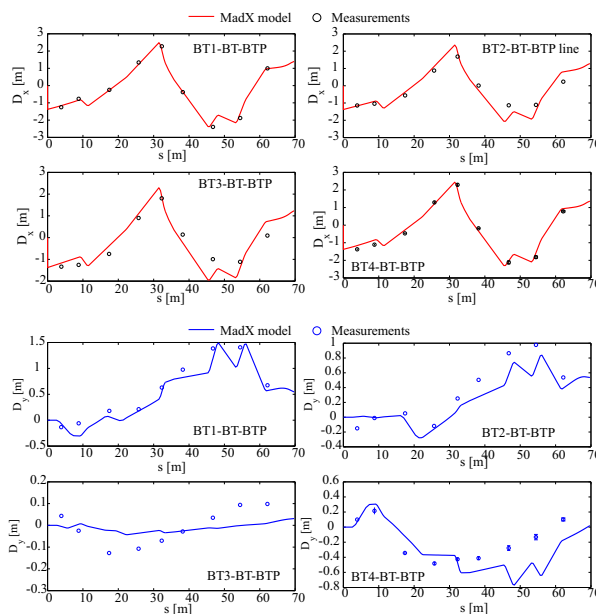


Figure 21: Dispersion in the BT i -BT-BTP lines (i represents the related PSB ring): measurements (circles) vs. MadX model (solid line) for the horizontal (top) and vertical (bottom) planes.

Conclusions of the MD

The PS first-turn horizontal dispersion was reduced from 5 m to ~ 2.5 m peak-to-peak, as shown in Fig. 22. This improvement, to date, did not affect the measured horizontal emittance at PS injection. Further efforts are on-going to better match the optics model of PSB-BT-BTP-PS with the measurements and validate its operational deployment for the 4 PSB rings, starting from ring 3.

MD1829 AND MD1893: TRANSFER OF LONG BUNCHES AND EMITTANCE EVALUATION

LHC "long" bunches (220 ns total bunch length, $(\delta v/v)_{rms} = 1.9 \times 10^{-3}$ and 3 eVs longitudinal emittance)

Table 4: Strengths of BT quadrupoles (operational and re-matched optics)

BT quadrupole	Operational strength [m ⁻²]	Scaling factor for re-matching
kBTQNO10	-0.66749	0.98
kBTQNO20	0.63160	1.02
kBTQNO30	-0.28709	0.94
kBTQNO40	0.92347	1.08
kBTQNO50	-0.73445	1.05

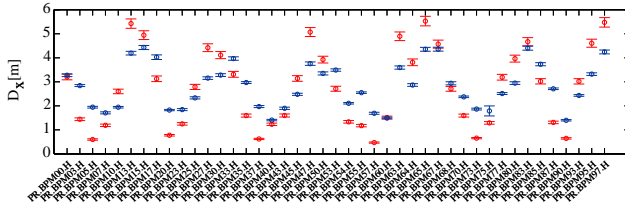


Figure 22: The measured horizontal dispersion (PS 1st turn from PSB ring 3) before (red) and after (blue) the correction.

were produced in the PSB and extracted to the PS [18]. The advantage of these bunches, with respect to the nominal 180 ns LHC bunches, is the increment of longitudinal emittance which leads to a 10% higher bunching factor at injection in the PS and, thus, a reduced transverse space charge tune spread.

The purpose of the MDs was to evaluate the transmission from PSB extraction to PS injection (MD1829) and the emittance growth at PS injection (MD1893).

The length of the bunches required a fine tuning of the recombination kickers fine delays, as the time margins were drastically reduced because of the new bunch lengths and same bunch spacings with respect to the 180 ns bunches [7].

The transmission, shown in Fig. 23, was optimised. Slow losses are still present along the flat-bottom, probably due to interaction with magnetic resonances.

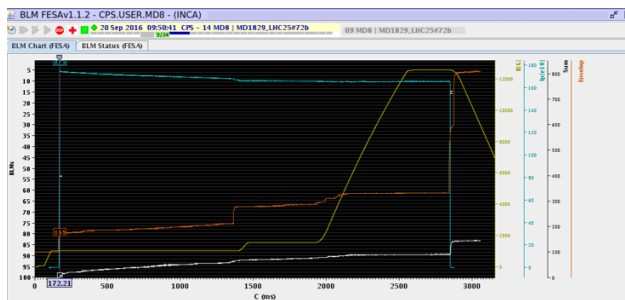


Figure 23: Single “long” bunch transmission in the PS.

The emittance evaluation was performed, in the horizontal plane, with the two wire scanners 65H and 54H. Unfortunately, probably due to the large momentum spread, the two instruments gave completely different values, as shown in Fig. 24. For this reason the topic needs further investigations in 2017.

During this MD, a peak line density increase was identified and correlated to a transverse space charge tune spread enhancement and consecutive vertical emittance growth during the transition from flat-bottom to intermediate flat-bottom (at around 1380 ms). Figure 25 shows the identified increase.

This finding was fundamental to improve the RF program and reduced the vertical emittance growth at flat-bottom of around 15% [15].

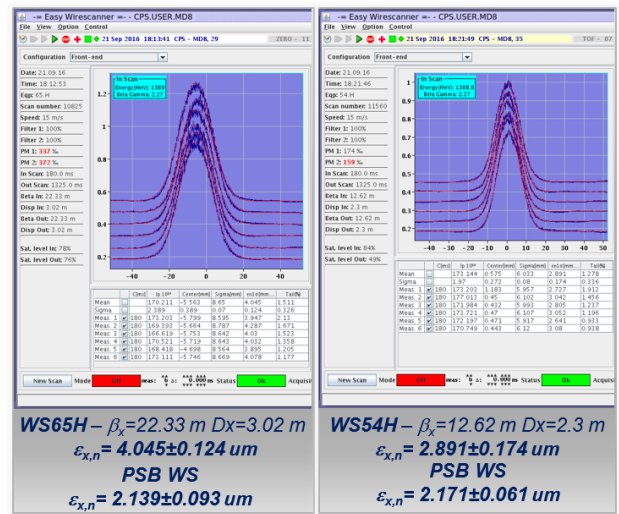


Figure 24: Different horizontal emittance evaluations from two PS wire scanners.

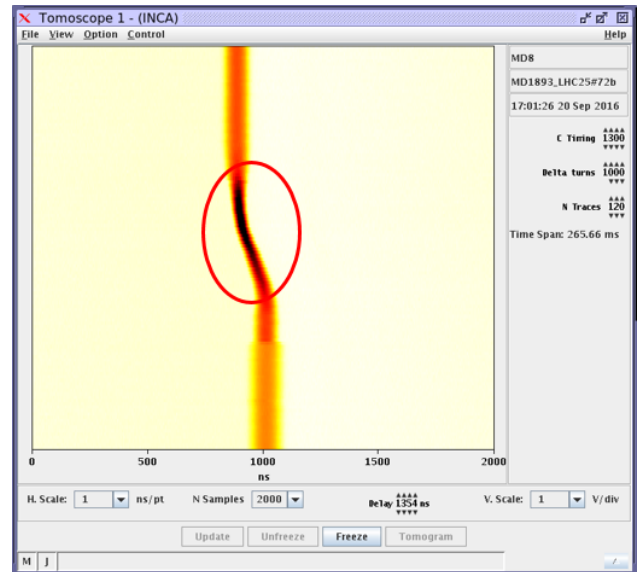


Figure 25: Longitudinal waterfall plot around the peak line density increase (in the red ellipse). Longitudinal density color-code: yellow - low particle density; black - high particle density.

Conclusions of the MD

The transfer of “long” bunches for LHC Standard production was performed successfully. Slow losses at PS flat-bottom energy have to be further investigated.

The emittance growth evaluation was stopped by the observation of different measurements from two horizontal PS wire scanners which also require further investigations.

A very important finding was the identification of the peak line density increase during the passage from flat-bottom to intermediate flat-bottom, which led to a 15% vertical emittance growth reduction for LHC beams.

MD1928: PS SEM-GRIDS AFTER INJECTION

The three SEM-grids in the PS sections 48, 52, 54 are named, respectively, PI.BSF48, PI.BSF52 and PI.BSF54. They are located after PS injection and represent important instruments in order to verify the LHC beams optics matching. These SEM-grids were unused for many years, so first purpose of the MD was their revival and functionality checks. A low intensity beam (LHCINDIV) was used.

The SEM-grids were used during a dedicated MD time. Parallel operation is not possible as they are moved by slow motors and need to work together with a device, called “ralentisseur”, which grants the single-passage of the beam, stopping it after it crosses the three SEM-grids. Multi-passage could, in fact, cause grid damage, especially for high intensity beams.

The SEM-grids have been verified and working. Dispersion measurements were performed. Further measurements will follow in 2017 in order to verify the transfer line with the 3-screens method [19].

MD1769: Automatic bunch alignment at PS injection

The 4 bunches coming from the PSB to the PS must be aligned in order to enter in the PS with the same trajectory. This process is usually performed by the operators in control room through the YASP program [20] and empirical approach.

An automatic tool developed by D. Gamba, called “linear feedback” [21], was adapted to try and align the 4 bunches to the beam dump in a semi-automatic way. The tool is capable of calculating on-line the response matrix and impose, in feedback, the right correction to the steerers in order to minimise the error in the alignment. The tool showed impressive potential, being capable of aligning the 4 bunches in the order of 0.5 mm. Further investigations switching the beam toward the PS are necessary in 2017.

MD1740: Septum SMH42 position and angle upgrade for LIU

This important MD was performed in order to verify if the new position and angle of the injection septum proposed to reduce injection losses of high intensity beams to the PS are feasible and do not disturb operation. The results were successful. More details are presented in [22].

CONCLUSIONS AND OUTLOOK

Many MD studies were carried out in 2016 for the beam transfer from the PSB to the PS, covering a wide amount of topics. The main ones concerned the PSB extraction at 160 MeV, the introduction of new methodologies for magnetic waveform measurements of kickers, dispersion measurement and re-matching between the PSB and the PS, transmission of long bunches and identification of a peak line density increase during the PS cycle, which was directly connected to a vertical emittance blow-up due to the transverse space charge tune shift enhancement.

Further investigations are planned for 2017. In particular:

- Improve re-matching of BT line optics (for Ring 3) in order to provide a matched optics and assess the impact of dispersion mismatch on emittance growth;

- evaluation of PS injection oscillations and injection bump non-closure with the aim to understand the shot-by-shot stability;
- quantification of the betatron mismatch at PS injection and analyse impact on emittance growth;
- repetition of KFA45 waveform measurements with the new hardware;
- improvement of the automatic steering technique to the PS;
- turn-by-turn SEM-grid measurements (when fast electronics is ready) in order to disentangle optics-related effects (faster) and space charge effects (slower) in emittance growth.

ACKNOWLEDGEMENTS

The authors would like to thank the PSB and PS OP teams for the important support.

REFERENCES

- [1] The LIU project: <https://espace.cern.ch/liu-project/default.aspx>
- [2] V. Forte *et al.*, Requirements and timeline for beam commissioning activities to operational beam, Linac4-PSB 160 MeV connection readiness review, 30/08/2016, <https://indico.cern.ch/event/548092/timetable>
- [3] W. Bartmann, PSB extraction at 160 MeV, LIU-PSB Meeting No. 56 (presented by B. Mikulec), <https://indico.cern.ch/event/160787>
- [4] F. Chapuis, “Booster Layout Drawings”, CERN EDMS: 492340
- [5] V. Forte, W. Bartmann, J.C.C.M. Borburgh, M.A. Fraser, L. Sermeus, “Beam-Based Kicker Waveform Measurements Using Long Bunches”, IPAC17 proceedings, Copenhagen, Denmark, MOPIK042
- [6] W. Bartmann *et al.*, “Specification for Kicker Systems For 2.0 GeV PSB to PS Beam Transfer”, CERN EDMS: PS-MKKIK-ES-0001
- [7] V. Forte, M. A. Fraser, W. Bartmann, J. Borburgh, L. Sermeus, “New beam-based and direct magnetic waveform measurements of the BTx.KFA10(20) vertical recombination kickers and induced emittance blow-up simulations at 1.4 and 2 GeV”, CERN-ATS-NOTE-2017
- [8] S. Deghaye *et al.*, “OASIS: A New System To Acquire And Display The Analog Signals For LHC”, Proceedings of ICALPCS2003
- [9] V. Forte, W. Bartmann, J.C.C.M. Borburgh, L.M.C. Feliciano, A. Ferrero Colomo, M.A. Fraser, T. Kramer, L. Sermeus, “Beam-Based Waveform Measurements of the CERN PS Injection Kicker”, IPAC17 proceedings, Copenhagen, Denmark, MOPIK043
- [10] J. Belleman, <http://jeroen.web.cern.ch/jeroen/tfpu/>
- [11] K.-D. Metzmacher, L. Sermeus, The PS Injection Kicker KFA45 Performance for LHC, PS/PO/Note 2002-015 (Tech.)
- [12] T. Kramer, Upgrade of the PS Injection Kicker KFA-45 for Operation with 2.0 GeV LIU Beams, CERN EDMS: PS-MKKFA-EC-0001 v.0.1

- [13] W. Bartmann, V. Forte, M.A. Fraser, "Emittance Growth at PS According to Model", CERN MSWG Meeting No. 15, 2016.
<https://indico.cern.ch/event/578789/>
- [14] G.P. Di Giovanni, V. Forte, G. Guidoboni, "Status of the PSB-to-PS transfer of long bunches preparation studies: BTM line SEM grid measurements", , CERN MSWG Meeting No. 15, 2016.
<https://indico.cern.ch/event/578789/>
- [15] H. Bartosik, "Emittance growth", CERN Injector MD Days 2017,
<https://indico.cern.ch/event/609486/>
- [16] PSB to PS optics:
<http://project-ps-optics.web.cern.ch/project-PS-optics/cps/TransLines/PSB-PS>
- [17] The MadX code: cern.ch/mad
- [18] S. Albright, "Longitudinal emittance blow up and production of future LHC beams", CERN Injector MD Days 2017,
<https://indico.cern.ch/event/609486/>
- [19] G. Arduini, M. Giovannozzi, D. Manglunki, M. Martini, "Measurement of the Optical Parameters of a Transfer Line Using Mutli-Profile Analysis", CERN PS (CA) 98-032 (1998).
- [20] The YASP steering program:
<https://jwenning.web.cern.ch/jwenning/documents/YASP/YASL-user-guide.pdf>
- [21] D. Gamba, F. Tecker, "Emittance Optimisation In The Drive Beam Recombination Complex at CTF3", Proceedings of IPAC14, Dresden, Germany, TUPRI080
- [22] M. Serluca, W. Bartmann, V. Forte, M. Fraser, G. Sterbini, "Injection Septa Position and Angle Optimisation in View of the 2 GeV LIU Upgrade of the CERN PS", *these proceedings*